

Strongly Correlated Electrons in Catalysis: Focus on Quantum Exchange

Chiara Biz,^{a,b} Mauro Fianchini,^a Jose Gracia^{a}*

^a MagnetoCat SL, General Polavieja 9 3I (03012), Alicante, Spain.

^b Universitat Jaume I, Av. Vicente Sos Baynat s/n, E-12071 Castellón de la Plana, Spain

* jose.gracia@magnetocat.com

KEYWORDS: strongly correlated electrons; quantum exchange interactions; quantum excitation interactions; spintro-catalysis; magneto-catalysis.

ABSTRACT: The understanding of quantum correlations within catalysts is an active and advanced research field, absolutely necessary when attempting to describe all the relevant electronic factors in catalysis. In our previous research we came to the conclusion that the most promising electronic interactions to improve the optimization of technological applications based on magnetic materials are Quantum Spin Exchange Interactions (QSEI), non-classical orbital mechanisms that considerably reduce the Coulomb repulsion between electrons with the same spin. QSEI can stabilize open-shell orbital configurations with unpaired electrons in magnetic

compositions. These indirect spin-potentials significantly influence and differentiate the catalytic properties of magnetic materials. As a rule of thumb, reaction kinetics (thus catalytic activity) generally increases when inter-atomic ferromagnetic (FM) interactions are dominant, while it sensibly decreases when antiferromagnetic (AFM) interactions prevail. The influence of magnetic patterns and spin-potentials can be easily spotted in several reactions, including the most important bio-catalytic reactions like photosynthesis, for instance. Moreover, we introduce here the concept of Quantum Excitation Interactions (QEXI) as a crucial factor to establish and influence the band-gap in materials and as a key factor to efficiently mediate electron transfer reactions. In the present perspective we offer a general conceptual overview, mainly based on our recent research, on the importance of strongly correlated electrons and their interactions during catalytic events. We present the physical principles and meanings behind quantum exchange in a way that facilitates a comprehensive understanding of the electronic interactions in catalysis from their quantum roots; we explore the issue *via* mathematical treatment as well as *via* intuitive visual space/time diagrams to expand the potential readership beyond the domain of physicists and quantum chemists.

1. Introduction

Strongly correlated electrons enhance the activity of certain catalysts; understanding “why” and “how” is strictly dependent on understanding complex quantum phenomena, like metal-insulator transitions and ferromagnetism.^{1,2} An improved fundamental view of the quantum electronic interactions (correlations)³ lets us uncover additional details of the most relevant quantum electronic factors in catalysis, their origin, nature and influence. The importance of this fundamental research on orbital magnetism and spin-potentials is not only confined to a pure

academic scientific domain, but, being deeply intertwined, as it is, with the efficiency of electrocatalytic processes and technologies for the production of “green” hydrogen, it bears a tremendous impact on the idea of a cleaner and more sustainable world.

1.1 The bumpy motion of electrons in orbitals.

The Coulomb potential between two particles with finite charge cannot grow infinitely as they approach since quantum mechanics corrects this classical singularity. The Coulomb field oscillates creating interference patterns as the charges move in space-time; for instance, the attraction between the hydrogen nucleus and its electron at distances smaller than the Bohr radius creates more destructive interferences. Forces are not always fixed in space-time as classical mechanics describes; thus, it results that the movements of electrons follow many possible paths because of the quantization of the electromagnetic field. “In their space-time evolution, electrons make that the forces, which determine their movement, waver”.⁴ The overall contribution of a path is proportional to $e^{iS/\hbar}$,⁴ where S is the action given by the time integral of the Lagrangian along the path.

Collisions. Electrons in orbitals follow intricate space-time trajectories, despite our inability to assess exactly where and when. They may also collide in scattering events. All this information is implicitly contained in the integrals derived from the Schrödinger's equation, in agreement with the Dirac factor $e^{iS/\hbar}$. Consequently, the Schrödinger (nonrelativistic) approximation, commonly used to understand the electronic factors in catalysis, includes all the events contained within the equivalent path integral description with an infinity of quantum-mechanically possible trajectories.³

1.2 Relativity, Quantum Mechanics and the Pauli exclusion principle: Origin of the Spin correlation.

The momentum p^{e-} of a free electron moving at velocity u in the observer's frame is $p^{e-} = m_0^{e-} \cdot \gamma \cdot u$ in special relativity, where $\gamma = \frac{1}{\sqrt{1-(\frac{u}{c})^2}}$, c is the speed of light and m_0^{e-} its rest mass.^{5,6} The

total energy of the electron is $E_+^{e-} = +\sqrt{(p^{e-} \cdot c)^2 + (m_0^{e-} \cdot c^2)^2}$. In order to incorporate the relativistic energy of an electron, Dirac obtained a wave equation that puts together Quantum and Relativistic Mechanics by introducing the $[\alpha_{x,y,z}]^{e-}$ and $[\beta]^{e-}$ matrices in the wave function $([\alpha_{x,y,z}]^{e-} \cdot c \cdot \hat{p} + [\beta]^{e-} \cdot m_0^{e-} \cdot c^2) \cdot \Psi^{e-} = \hat{E} \Psi^{e-}$. The evaluation of Ψ^{e-} for the free electron gives two solutions with the same positive energy, interpreted as spin degrees of freedom. It

follows that a free electron has two states with different spin and the same energy, $\Psi_{+\alpha}^{e-} = \begin{bmatrix} 1 \\ 0 \\ 0 \\ 0 \end{bmatrix}$.

$e^{-i/\hbar \cdot |E^{e-}| \cdot t}$ and $\Psi_{+\beta}^{e-} = \begin{bmatrix} 0 \\ 1 \\ 0 \\ 0 \end{bmatrix} \cdot e^{-i/\hbar \cdot |E^{e-}| \cdot t}$, even for the simplest solutions. Thus, Dirac spinors

provide a complete and orthogonal set of solutions. As a consequence, of the combination of

special relativity and quantum mechanics, chemistry, thus catalysis, developed the notion of the spin degree of freedom.

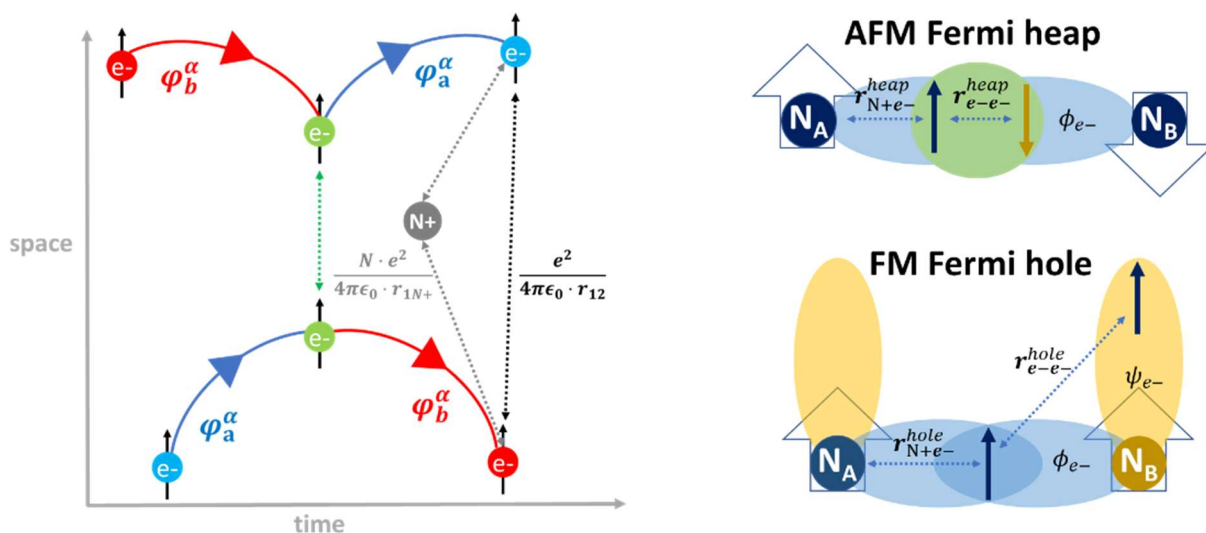


Figure 1. Left Space-time diagram representing the Quantum Spin Exchange Interaction between two electrons with the same spin in the molecular orbitals φ_a^α and φ_b^α . Electrons are described by an anti-symmetric wavefunction, resulting in either a Fermi hole in ferromagnetic (FM) bonds with orthogonal electrons having a lower probability of being found close to each other (bottom right) or a Fermi heap, in overlapping antiferromagnetic (AFM) couplings having a higher probability of being localized close to each other (top right).

Orbital magnetism in principles emerges as a quantum phenomenon, because of the requisite of forming antisymmetric wavefunctions ($\Psi_{e-}^{\text{antisym.}}$) versus the permutation of the indistinguishable electrons (fermions).³ Two electrons with the same spin cannot occupy simultaneously the same orbital (hence they result spin-correlate), otherwise the wavefunction probability amplitude is zero. The $\Psi_{e-}^{\text{antisym.}}$ solutions mathematically introduce Quantum Spin Exchange Interactions (QSEI) as integral energy terms that may be understood in the path formulation as scattering events occurring inside electronic configurations. We developed particular Feynman's type diagrams for the dynamic behavior of electrons in atoms. Figures 1 left and 2a show QSEI as space-time scattering events only accessible among electrons with the same spin.³ The figures explain that two electrons, one in the orbital ϕ_a^α and the other in the ϕ_b^α (y-axis), initially distant at time 0 (x-axis, left), start approaching each other at time t (x-axis, center). At this time their repulsive Coulomb potential increases, yet, the repulsion cannot grow indefinitely since the electrons are in a quantized field at any point and instant. Thus, the system allows that the electrons interchange their orbitals (again, time t, center) and energy-momentum, avoiding each other in order to decrease the repulsion between them. The net result of this mechanism at time final (x-axis, right) is that the electrons exchanged their orbitals. What we are describing here is the same mechanism that allows electrons with the same spin to actually be indistinguishable particles. Thus, under this perspective, it turns out that QSEI are quantum mechanisms that electrons with the same spin use to avoid proximity (i.e., a spin correlated movement in their multifaceted orbital movements). At this moment, we would like also to clarify that QSEI is not the mechanism that determines directly the electric conductivity,⁷ since electrons in the Highest Occupied Bands (HOBAs) can still feel a strongly localizing potential and an energy gap may exist towards the Lowest Unoccupied Bands (LUBAs). We will argument more about the conduction band in section 1.3.

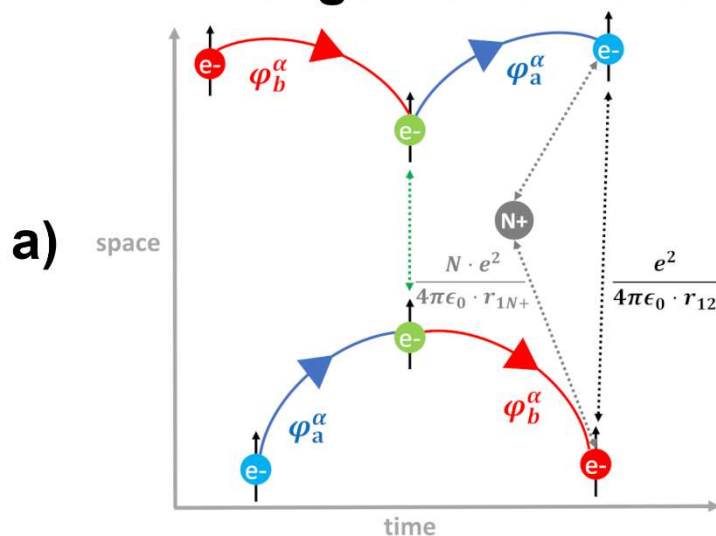
QSEI are ubiquitous and significant in both closed-shell and open-shell catalysts. They are however especially relevant for configurations with unpaired electrons.⁸ Their understanding is essential for the full comprehension of the specific properties of magnetic structures (with Fermi heaps and holes, Figure 1 right). QSEI are a spin-dependent part and the most important among the correlation mechanisms in orbital physics, a significant contribution that can reshape the energy, orbital and catalytic structure; thus, a relevant factor that affects bond breaking and formation,^{9,10} as well as ionic and electron transport.¹¹

We are mentioning the existence of two other magnetic potentials that are very relevant in catalysis for completeness of treatment, even though we will not analyze them in details here: direct spin-spin interactions (DSSI, bottom left of Figure 2),¹² and strong spin-orbit couplings specially in chiral structures (CISS, bottom right of Figure 2).^{13,14,15} These three spin-dependent potentials, QSEI, DSSI and CISS, share a common acting principle: increasing stabilization *via* decreasing electronic repulsions. This spin-induced magnetic stabilization bears a great impact in catalytic events, especially those associated with delocalized Charge, Spin and Fermi holes.¹ These magnetic interactions are also inevitably entangled: once DSSI or CISS potentials stabilize a magnetic structure, the repulsions among spin-oriented electrons in the structure decrease due to internal QSEI. To be extremely pragmatic, we could infer that this DSSI(external)-QSEI(internal) “entanglement” is exactly what happens when catalytic reactions based on magnetic structures are forced to run in presence of external magnets.^{8,12}

Theory predicted that indirect QSEI are typically stronger than the direct spin-spin potentials.^{8,16} There are already plenty of experimental evidences in literature corroborating the success of theoretical analyses that include spin-potentials as the most significant part of the electronic correlations in catalysis.^{17,18,19,20,21,22,23,24,25,26,27,28} This analysis, embedding a full quantum

mechanic treatment, corrects and complements other non-correlated approximations, like the d-band model, only sufficiently accurate for systems with weakly correlated electrons.²⁹

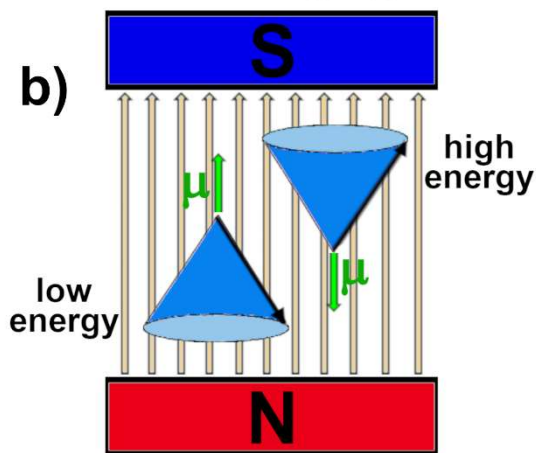
Exchange Interactions



Catalysts with Dominant Ferromagnetic Couplings

Spin-Spin Interactions

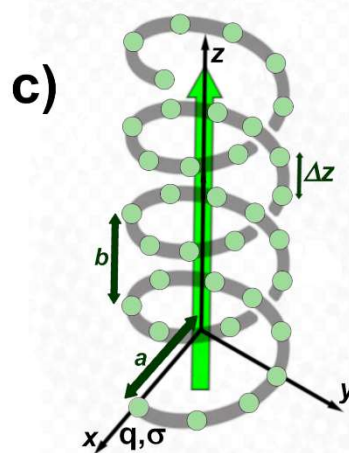
$$\mu = -gm_S\mu_B$$



External Magnetic fields

Spin-Orbit Couplings

$$E_{\text{helix}} \rightarrow B = (v/c^2) \times E_h$$



Chiral Catalysts

Figure 2. Representation of three kinds of relevant spin-dependent potentials in catalysis.

1.3 Quantum Excitation Interactions (QEXI).

A Slater determinant is an antisymmetric wavefunction representing the occupation of a single electronic configuration, the most stable being $|\Phi_0\rangle$. If we introduce $|\Phi_0\rangle$ as solution to the Schrodinger equation, $\hat{H} \cdot |\Phi_0\rangle = E_0^{Hartree-Fock} \cdot |\Phi_0\rangle$, we will get the Kinetic and Coulomb energy of the electron and QSEI. This solution, however, neglects the Quantum Excitations Interactions (QEXI).⁷ The previous physical description conveys the idea that $E_0^{Hartree-Fock}$ is the energy for $|\Phi_0\rangle$ (a single Slater determinant) if the electrons will always be confined in space-time exclusively in a single electronic structure, for instance $1S^2 = |1^\alpha 1^\beta\rangle$ for the He atom.

In reality the ground state (G.S.) is a combination of more than a single electronic configuration, since the electrons undergo temporary excitations to reduce their mutual Coulomb repulsions.³ If we improve the G.S. function *via* a linear expansion of the most stable electronic configurations, including all the possible excitations, then we have that: $|\Psi_0\rangle = c_0 \cdot |\Phi_0\rangle + c_1 \cdot |S\rangle + c_2 \cdot |D\rangle + c_3 \cdot |T\rangle$ and so on, where $|S\rangle$, $|D\rangle$ and $|T\rangle$ represent terms involving single, double and triple excitations (and so on). Using this expansion, we can get the exact energy ($E_{G.S.} = E_0^{Hartree-Fock} + E_{QEXI}$). Thus, the Quantum Excitations Interactions represent the Correlation Energy.

Electrons in the G.S. of a certain system can be excited into excited electronic configurations (essentially orbitals with higher energies) and thus reduce their total energy. In order to understand the subtleties of this issue, let us start with a small mathematical description of the most basic model for He. We include only the $1S^2 = |1^\alpha 1^\beta\rangle$ and the $2S^2 = |2^\alpha 2^\beta\rangle$ configurations in the G.S. in order to have the spin-adapted singlet state expansion $|\Psi_0^{He}\rangle = c_{1s2} \cdot |1^\alpha 1^\beta\rangle +$

$c_{2s2} \cdot |2^\alpha 2^\beta\rangle$. Only these two configurations are available. Since electrons are confined in space-time in them, then we can normalize the wave-function as $(c_{1s2})^2 + (c_{2s2})^2 = 1$. The energy is $E_{G.S.}^{He} = \langle \Psi_0^{He} | \hat{H} | \Psi_0^{He} \rangle$:

$$E_{G.S.}^{He} = (c_{1s2})^2 \cdot \langle 1^\alpha 1^\beta | \hat{H} | 1^\alpha 1^\beta \rangle + (c_{2s2})^2 \cdot \langle 2^\alpha 2^\beta | \hat{H} | 2^\alpha 2^\beta \rangle + 2 \cdot c_{1s2} \cdot c_{2s2} \cdot \langle 1^\alpha 1^\beta | \hat{H} | 2^\alpha 2^\beta \rangle$$

If $(c_{1s2})^2 = 1$, then $E_{G.S.}^{He} = E_{1s^2}^{single-configuration}$; conversely, if $(c_{2s2})^2 = 1$, then $E^{He} = E_{2s^2}^{single-configuration}$. Since $E_{1s^2}^{single-configuration} < E_{2s^2}^{single-configuration}$, these two isolated configurations will give a G.S. with $(c_{1s2})^2 = 1$ and $(c_{2s2})^2 = 0$. $E_{QEXI}^{He} = 2 \cdot c_{1s2} \cdot c_{2s2} \cdot \langle 1^\alpha 1^\beta | \hat{H} | 2^\alpha 2^\beta \rangle$ is an additional stabilizing term, since both configurations participate together in the space-time movement of electrons.

$$E_{QEXI}^{He} = -2 \cdot c_{1s2} \cdot c_{2s2} \cdot K_{12} = -2 \cdot c_{1s2} \cdot c_{2s2} \cdot \left\langle \psi_{1s} \psi_{2s} \left| \frac{1}{r_{12}} \right| \psi_{2s} \psi_{1s} \right\rangle$$

K_{12} is the quantum exchange integral and ψ_{1s} and ψ_{2s} are the spatial orbitals in He. The dependence of the E_{QEXI}^{He} versus the occupation of the two configurations, coefficients c_{1s2} and c_{2s2} , is not linear. If c_{1s2} is slightly smaller than 1 and c_{2s2} is slightly bigger than 0, then the term E_{QEXI}^{He} decreases the total energy. The coefficient c_{1s2} must still be very close to 1, otherwise the contribution $(c_{1s2})^2 \cdot \langle 1^\alpha 1^\beta | \hat{H} | 1^\alpha 1^\beta \rangle + (c_{2s2})^2 \cdot \langle 2^\alpha 2^\beta | \hat{H} | 2^\alpha 2^\beta \rangle$ increases the total energy (for its quadratic dependency). In other words, the minimum energy of the system is found for $c_{1s2} < \sim 1$ and $c_{2s2} > \sim 0$. In such situation both orbital configurations participate in the G.S. and electrons use excited configurations to reduce their total energy in the space-time movement.

Figure 3 shows a space-time view of this simplest excitation mechanisms that contribute to Quantum Excitation Interactions (QEXI) in He. We should remember that, according to Brilluoin's

theorem,⁷ the Configuration Interaction matrix elements from singly excited configurations will be very weak), so, according to this, the simplest and more relevant QEXI in this example is a double excitation (Figure 3). We proceed to describe Figure 3 as we described Figure 1. Two electrons occupy two spatial orbitals, φ_a (y-axis), at time 0 (x-axis, left). At time t (x-axis, center), they get in close proximity so that their mutual Coulomb repulsion temporally increases to the point that both jump into excited and more diffused orbitals, φ_r . This way the growing Coulomb repulsion diminishes. Once the electrons separate further in space-time, the electrons relax back to the most stable configuration, at time final (x-axis, right). All these mechanisms are contemplated in the electronic ground state. QEXI are simply linked with the transient occupation of empty diffuse orbitals by excited electrons. As in the case of QSEI, QEXI are scattering mechanisms associated with electron dynamics mainly represented with exchange integrals (further details in section 2).

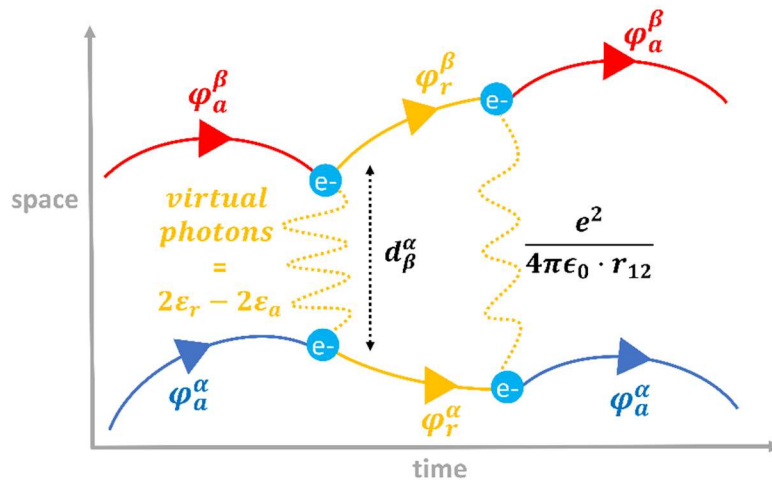


Figure 3. Space-time diagram that represents a Quantum Excited Interaction between two electrons initially in the molecular orbital ϕ_a^α . When the electrons get in close proximity, both jump temporarily into an excited and more diffused orbital ϕ_r^α .

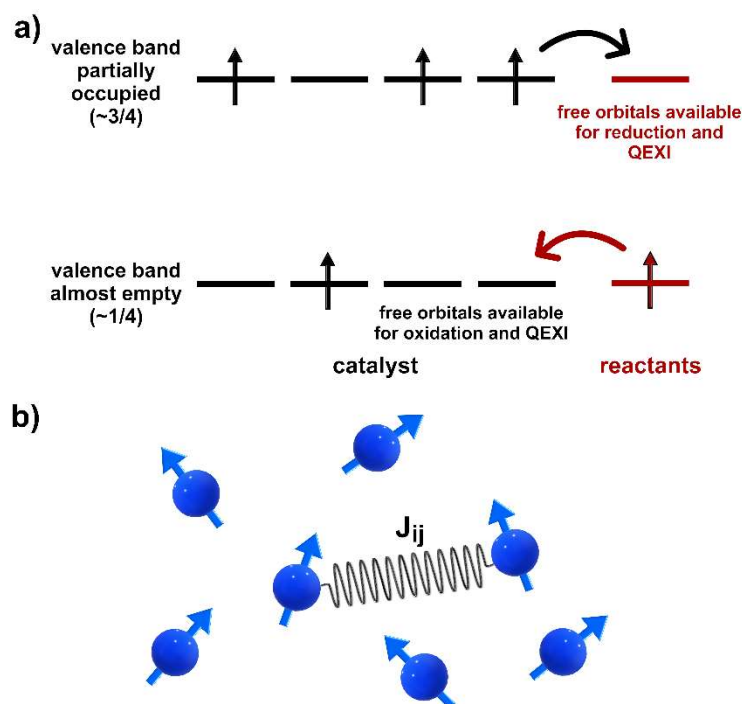


Figure 4. *a) QEXI help to place electrons from semi-occupied valence band of the catalyst (3/4) into empty orbitals of the reactant or, vice-versa, from occupied orbitals of the reactant into empty valence band of the catalyst(1/4). b) Schematic representation of the QSEI still present above the Curie temperature.*

The “empty” orbitals (i.e., excited electronic configurations) constitute the conduction band in materials. Thus, we can draw a very important conclusion in the context of electrocatalysis: QEXI help in the electronic mobility. Unfortunately, obtaining a full description of the QEXI in catalysis is nowadays still a big challenge, because computation should rely on multi-configurational approaches.³ Nonetheless, we can already outline two factors where QEXI play a role in electrocatalysis. Electron transfer reactions use the empty orbitals of the conduction band^{1,2} for enhanced electron transport, as described in previous studies.^{30,31} This is non-trivial, however, because an underestimation (or even neglect) of QEXI term in calculations, will lead to an

inevitable overestimation of the E_{gap}^{band} and to an exponential overestimation of the activation energy ($e^{-E_{gap}^{band}/k_B T}$).

Another factor, where we anticipate that QEXI play an important role in electrocatalysis, is the selectivity. Valence bands that are partially occupied, but almost filled ($\square 3/4$ occupancy), are more prone to reduction of the reactant (Figure 4a). On the other hand, if the valence bands are poorly occupied ($\square 1/4$ occupancy), the catalyst is more prone to oxidation of the reactant (Figure 4a). In both cases, there is an electronic entropic factor, associated with a preference in the sense of the current.

Given their nature, QEXI play a role in facilitating the excitation of electrons, carrying, as we saw, a certain degree of implicit selectivity. As of yet, the quantification of such mechanisms is outside of the scope of our perspective, whose goal is uniquely to provide a space-time picture of QEXI for a better fundamental understanding. Let us finish this section mentioning that the manipulation of QEXI for the rational design of improved catalysts is but, in its infancy, to our knowledge.

1.4 Outline of QSEI in catalysis.

The relative relevance of the energy terms derived from QSEI varies between non-magnetic and magnetic systems. Particularly, the on-site (intra-atomic) electronic Coulomb repulsions are strong within the compact **3d** and **4f** frontier orbitals of metals and this can lead to configurations with unpaired electrons ($QSEI_{shells}^{open}$). In addition, if we acknowledge the presence of several magnetic centers connected by covalent bonds, as it is in magnetic materials, cooperative inter-atomic $QSEI_{shells}^{open}$ shape the overall complex magnetic, electric³² and catalytic properties.

Predominant inter-atomic antiferromagnetic (AFM) orbital orderings lead to electronic localization in the space (strongly localized Fermi heaps), occurring between magnetic metal centers (as previously shown in Figure 1 right (top) and Figure 8 center): the spins of neighboring magnetic centers point in opposite directions. Instead, as shown in Figure 1 right (bottom) and Figure 8 right, predominant inter-atomic ferromagnetism (FM), also present in ferrimagnetic and layered AFM type-A couplings) needs an excess of empty orthonormal **3d**-orbitals close in energy. The partial orbital filling of the frontier FM covalent bonds allows the spins of the magnetic metals to point in the same direction.^{33,34} Previous description prevails even above Curie temperature; fast electronic transitions, in fact, will still use the locally available FM spin delocalization even in presence of oscillations due to vibrations and/or disordered magnetic domains (Figure 4b).

In AFM couplings there are significant inter-atomic electronic repulsions among magnetic centers, compensated by stronger nuclei-electron attractions (Fermi heaps). In FM couplings electronic repulsions decrease in FM bonds due to the exchange delocalization in presence of an excess of $\text{QSEI}_{\text{shells}}^{\text{open}}$ at the valence band (Fermi holes).^{35,36,37}

After providing this previous general and basic analysis in sections 1.1, 1.2, 1.3 and 1.4, this perspective will focus on describing the impact of spin-dependent catalysis in “real life” experimental cases, in sections 1.5 and 1.6., and finally explaining the actual orbital physics and how this affects (electro-)catalysis, in section 2. We excluded from this perspective an extensive description of the cases where spin-dependent catalysis is very relevant in natural occurring biochemistry, even though the most important reactions for life depend on magnetic catalysts (i.e., photosynthesis). Natural selection exploits “spintro-biocatalysis” by making extensive use of $\text{QSEI}_{\text{shell}}^{\text{open}}$ in metals like Mn, Fe, Co and Cu, that are native in magnetic molecules devoted to

catalyze redox reactions^{38,21} and/or *via* chiral structures for spin-selection (Figure 2 - right).^{39,40,41,42,43} The specific term spintro-biocatalysis was suggested to us in a private communication by a past reviewer to explicitly distinguish the peculiarities of spin-dependent potentials in biocatalytic processes. We are using the term as it is here, an archetype that implies a combination of QSEI from open shell active centers and chirality in bioactive molecules.^{44,45}

1.5 Pure Transition Metals.

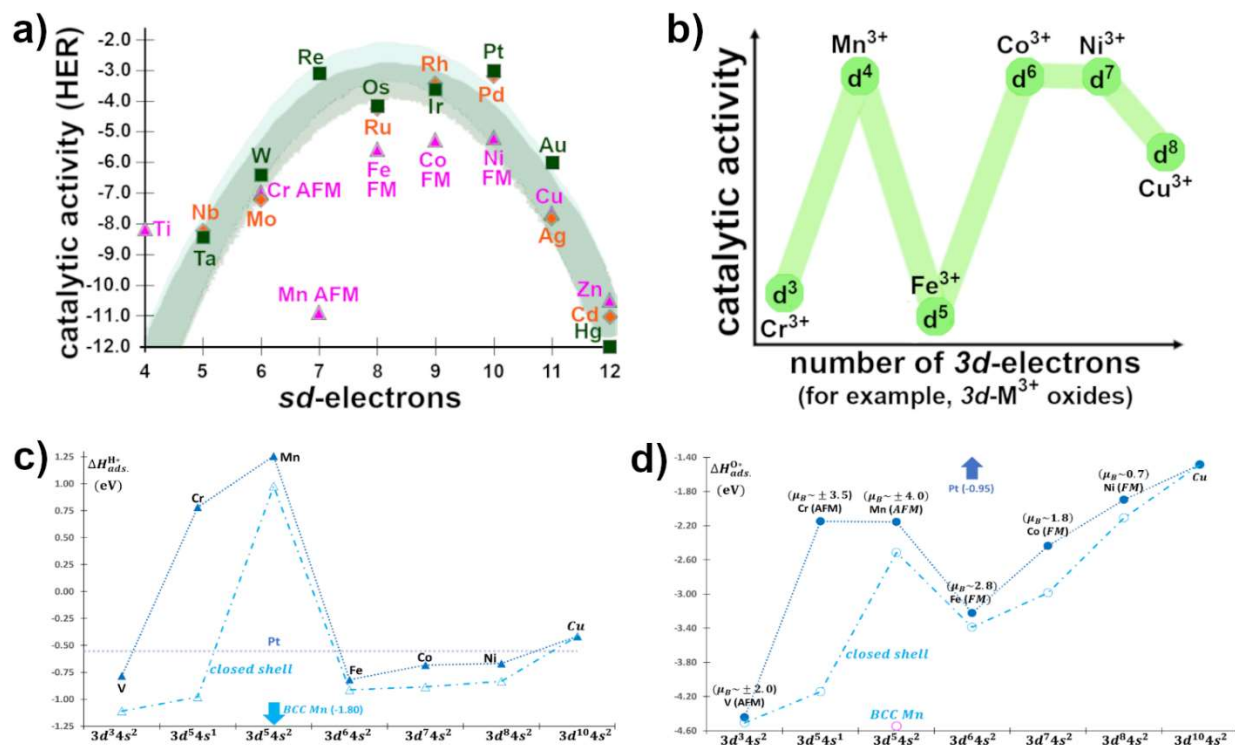


Figure 5. **a)** Current-activity versus the number of sd-electrons during hydrogen evolution reaction (HER) on transition metals.^{46,47} The data refer to similar acid conditions at room temperature. **b)** Qualitative representation of the activity trend versus the number of 3d-electrons adapted from experimental results on oxides.^{48,49,50} **c)** Calculated adsorption energies for hydrogen, ΔH_{ads}^{H*} and d) oxygen atoms, ΔH_{ads}^{O*} . The adsorptions are calculated versus gaseous H_2 and O_2 on equivalent close-pack surfaces of V, Cr, Mn, Fe (BCC (1 1 0) surface), α -Mn (100), Co (HCP (1 1 1) surface), Ni and Cu (FCC (1 1 1) surface) at 0.5 ML. Hollow markers correspond to non-physical closed-shells configurations.

The simple hydrogen evolution reaction (HER) on transition metals is quite revealing (Figure 5a); the experimental activity of closed-shell catalysts can be well encased into a single-volcano or

parabola plot versus the number of *sd*-electrons in the transition metals.^{46,47} However, under same conditions (e.g. oxidation state, structure), multi-peak drifts appear in catalysts based on *3d*-magnetic metals. Similar deviations due to magnetism are ubiquitously observed in pure *3d* metals,^{46,47} intermetallic alloys,⁵¹ carbides,⁵² oxides,^{53,54} sulphides⁵⁵ and nitrides⁵⁶ involved in different chemical transformations. The spin of the electron is a crucial factor to be considered in catalysis.^{57,58,59,60,61} The alternation of the spin structure of the transition-metals changes the adsorption/desorption energy of the active sites, Figure 5a, dramatically affecting the reaction thermodynamics.^{58,23,61}

The Oxygen Reduction Reaction (ORR) by the optimal FM Pt₃M alloys is another striking example^{62,63} where QSEI have a central role in the stabilization of the entire atomic structure. The best catalysts for cathodes in hydrogen fuel cells are Pt₃Co_{1-x}Ni_x nanostructures. The superior activity of these magnetic Pt-alloys, compared to metallic platinum, correlates with the milder chemisorption of the oxygenated intermediates on the surfaces of the alloy. QSEI, including interlayer exchange coupling due to magnetic inner layers, are determinant to make the active sites prone to bind adsorbed oxygen atoms in an optimal fashion for catalytic activity. These research advances^{62,63} predicted that a preferential multilayered structural organization for Pt₃Co (and related) is the reason for enhanced catalytic properties. Such structural features are already known for exhibiting specific magnetic properties, useful for exploitation in spintronics.⁶² This structure-magnetism-activity relationship represent an excellent *trait d'union* between heterogeneous catalysis and spintronics.⁶²

1.6 Transition Metal Oxides.

Early examples of spin effects in catalysis were mainly found on magnetic oxides and sulfides, where a close correlation was established between the spin state of the transition metals and their catalytic efficiency for OER.^{64,65,66,67} For example, Co^{3+} (d^6) exhibits both high spin state ($t_{2g}^4 e_g^2$) and low spin state ($t_{2g}^6 e_g^0$) under octahedra field, yet high spin Co^{3+} in a FM conductor shows higher OER activity than low spin Co^{3+} ,⁶⁶ confirming earlier predictions.^{68,69,2,1}

The spin polarization can also be created by vacancy engineering as demonstrated in TiO_2 with Ti defects at 0 ~ 30%.⁷⁰ It has been found that the spin polarization reaches the highest level in TiO_2 with Ti defects at 10%. This value provides the highest cell performance in photocatalysis. Spinel LiCoVO_4 with magnetically polarized lattice planes, that can provide spin channels for polarized spin transfer, reaches high OER efficiency.⁷¹

Our present comprehensive model can likewise explain the reduction in the overall cell energy consumption by using a NiFe-based (spin-polarized) catalyst by applying a magnetic field for CO_2 electrolysis.⁷² As we mentioned before, the main effect of the addition of an external magnetic field to a catalytic structure is to align the internal magnetic domains, macroscopically unifying internal QSEI (the stronger spin-potentials, as we previously mentioned) to reach optimal spin-catalytic conditions.

2. Theoretical Revision

2.1 Trends in non-magnetic catalysts.

Covalent solids with closed-shell configurations have all the electrons pairing their spins in orbitals. These configurations take full advantage of the Coulomb attractions, with valence

electron pairs ($\uparrow\downarrow$) sharing the space at inter-nuclear regions. Systems based on $4d$ and $5d$ orbitals are typically non-magnetic, because they have a larger radial extension than $3d$ and $4f$ orbitals and then the on-site electronic repulsions are not strong nor confined.^{73,74} In such cases, increasing Coulomb attractions is thus more favorable than reducing electronic repulsions via QSEI.

Table 1 shows the orbital electronic integrals, that determine the energy for any catalytic event on non-magnetic closed-shell surfaces, necessarily obtained from an anti-symmetric wavefunction.³ The electronic features of catalysis for non-magnetic materials, like covalent bonding and activation energies, do not show dependence upon spin-polarization. Approximations to catalysis based on the electronic contributions in Table 1 assume the energetics (thermodynamics) of the interactions between the active sites and the reaction intermediates as independent of the spin.^{75,76} Thus, spin-independent models should be only limited to this case and not universally applied.

The electronic energetic terms presented in Table 1 can be summarized as: the kinetic energy of every electron, $T_{e-}^{kinetic} > 0$, the Coulomb attraction between every electron and nuclei, $V_{N+e-}^{Coulomb} < 0$, the Coulomb repulsion within all electron pairs, $V_{e-e-}^{Coulomb} > 0$, the stabilizing QSEI between electrons with the same spin, $QSEI_{shel}^{closed} < 0$ and the excitation correlation, $QEXI < 0$.

Table 1. Most relevant quantum energy contributions related with energetic changes on non-magnetic catalysts. The wavefunction is based on Slater determinants, constructed from mono-electronic spin-orbitals (whose spatial part is ψ_a) as solution to the non-relativistic Schrödinger Hamiltonian for the valence electrons.

$$\Delta H_{cat.event}^{non-mag.} = \Delta T_{e-}^{kinetic} + \Delta V_{N+e-}^{Coulomb} + \Delta V_{e-e-}^{Coulomb} + \Delta QSEI_{shells}^{closed} + \Delta E_{e-}^{exc.corr.}$$

<i>Energy Factor</i>	<i>Integral Expression</i>
<i>Kinetic energy</i>	$\mathbf{T}_{\mathbf{e}^-}^{\text{kinetic}} = \sum_a^n \left\langle \psi_a \left -\frac{1}{2} \nabla^2 \right \psi_a \right\rangle$
<i>Coulomb nucleus-electron attractions</i>	$\mathbf{V}_{\mathbf{N}+\mathbf{e}^-}^{\text{Coulomb}} = - \sum_a^n \sum_A^N \left\langle \psi_a \left \frac{Z_A}{r_{1A}} \right \psi_a \right\rangle$
<i>Coulomb electron-electron repulsions</i>	$\mathbf{V}_{\mathbf{e}^-\mathbf{e}^-}^{\text{Coulomb}} = \sum_a^n \sum_{b>a}^n \left\langle \psi_a \psi_a \left \frac{1}{r_{12}} \right \psi_b \psi_b \right\rangle$
<i>Quantum Spin Exchange Interaction</i>	$\mathbf{QSEI}_{\text{shells}}^{\text{closed}} = - \sum_a^{n/2} \sum_{b>a}^{n/2} \left\langle \psi_a \psi_b \left \frac{1}{r_{12}} \right \psi_b \psi_a \right\rangle$
<i>Quantum Excitation Correlation</i>	$\mathbf{QEXI} = \mathbf{E}_{\mathbf{e}^-}^{\text{exc. corr.}}$

Closed-shells maximize the number of electron pairs, thus the electronic properties are not affected by the spin: the contribution of the $\mathbf{QSEI}_{\text{shells}}^{\text{closed}}$ stabilization terms is the minimum possible and do not accumulate at specific regions in position and momentum space. Figure 6 shows a simplified representation of the $\mathbf{QSEI}_{\text{shells}}^{\text{closed}}$ as dotted arrows between three closed-shells. We use a basic model limited to an orbital ψ_I mainly localized in a reaction intermediate and the two highest energy levels of the catalyst, ψ_a and ψ_b . The Coulomb repulsions, not explicitly indicated in Figure 6, are roughly providing twice the energetic contribution than the $\mathbf{QSEI}_{\text{shells}}^{\text{closed}}$ for non-magnetic materials, see the summations in Table 1.

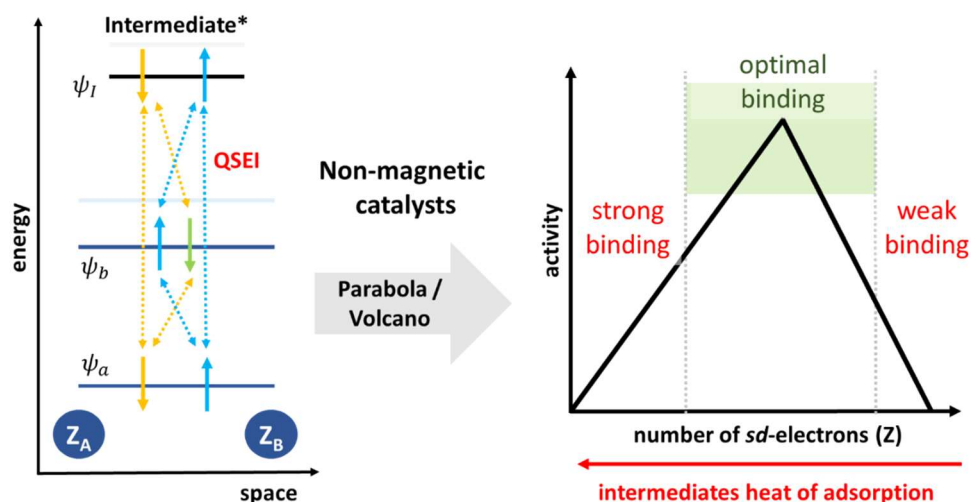


Figure 6. Left) Simplified energy/space plot for closed-shells catalysts and intermediates: blue and orange dotted arrows indicate the quantum spin exchange interactions (QSEI). Right) Volcano plot introduced by Balandin et al.⁷⁷

Plotting the energy of chemisorption for active metals along the same period versus the atomic number (Z) for closed-shell active sites leads to Volcano plots in catalysis as demonstrated by Balandin.⁷⁷ This is due to the consistent increase of the Coulomb repulsions $\Delta V_{e-e}^{Coulomb}(Z)$ versus the stabilizations $\Delta V_{N+e-}^{Coulomb}(Z) + \Delta QSEI_{shel}^{closed}(Z)$ as the energy shells fill up. Quasi-parabolic trends are typically observed in the HER activity for non-magnetic metals.⁷⁸ The hydrodesulphurization shows simple parabolic dependence versus the orbital-filling on transition metal sulphides.⁵⁵ Overall, non-magnetic metallic catalysts (weakly correlated systems) reasonably follow the band-theory and related models. Thus, the adsorption of substrates and activation energies are well-described by the d-band model of chemical bonding.⁷⁹ The reaction rates versus the occupation of the d-orbitals f_d (or Z) show a single volcano-peak that can be reasonably fitted by a parabola^{79,80} (introduced in Eq. 1).

In non-magnetic catalysts with increasing \mathbf{Z} , or $\mathbf{f_d}$, the higher relative stability of the electrons leads to an almost constant decrease of the adsorption energies, due to increasing electronic repulsions. Maximum catalytic activity appears for low-to-intermediate chemisorption energies, corresponding to a medium-high value of $\mathbf{f_d}$. The same reason explains why the cohesive energy of $4d$ - $5d$ metals grows until the d-shell is about half-occupied ($\sim d^5$) and then decays.⁷⁸

Eq. 1 is the simplest way to express the activation energy of a catalytic step as a function of the orbital occupation ($\mathbf{f_d}$ or \mathbf{Z}). Eq. 1 is an ideal expression (never fully accurate), where catalysts based on metals of the same period, with equal oxidation state and coordination, have equivalent “constant” electronic parameters \mathbf{a} , \mathbf{h} and \mathbf{k} for the activation energy of a chemical reaction. Once we know the physical meaning of these parameters, we can fit the experimental activities at the actual reaction conditions.

$$\text{Eq. 1) } \Delta H_{activation}^{non-magnetic}(\mathbf{f_d}) = \mathbf{a}(\mathbf{f_d} - \mathbf{h})^2 + \mathbf{k}$$

Sabatier’s principle remarks that the interactions must be “exactly right” for optimal reactivity. Thus, a low $\mathbf{f_d}$ value in Eq. 1 equates to excessive Coulomb attractions ($\Delta V_{N+e-}^{Coulomb} < 0$), that, in turn, translates into strong chemisorption of intermediates limiting the kinetics ($\Delta H_{activation}^{non-magnetic} \sim \mathbf{a}\mathbf{h}^2 + \mathbf{k}$). Conversely, a high $\mathbf{f_d}$ value equates to considerable electronic repulsions ($\Delta V_{e-e-}^{Coulomb} > 0$), that translates into poor activation of covalent bonds and weak (or endothermic) chemisorption, limiting once again the activity ($\Delta H_{activation}^{non-magnetic} \sim \mathbf{a}\mathbf{f_d}^2 + \mathbf{k}$). Thus, optimal reaction rates with low-to-medium covalent adsorption energies correspond to medium-to-high $\mathbf{f_d}$ values, closer to the \mathbf{h} of the reaction, where the terms $\Delta V_{N+e-}^{Coulomb}$ and $\Delta V_{e-e-}^{Coulomb} + \Delta QSEI_{shells}^{closed}$ terms are competing among each other.

The early work of Balandin and co-workers also showed another fundamental insight: a conspicuous number of catalytic transformations based on magnetic compositions for which single Volcano plots do not hold.⁷⁷

2.2 Multipeak volcano plots in magnetic catalysts.

The experimental activity trend of compositions based on *3d*-metals show significant oscillations and multiple peaks versus orbital filling (**fa**). The sudden deactivation of antiferromagnetic (AFM) Mn for HER, compared to its previous and following elements, is significant.⁸¹ A well-characterized deactivation of AFM MnS can be seen in hydrodesulphurization;⁵⁵ similar examples are AFM Fe³⁺ oxides in oxygen catalysis.^{48,82,83} The primary cause of this phenomenon is electronic, but that also includes structural changes. In a series of catalysts, abrupt changes in their properties occur with the magnetic ordering, from non-magnetic to dominant antiferromagnetic or (ferri-) ferromagnetic couplings. Predominant FM orbital orderings systematically deliver optimal catalysts for the oxygen evolution reaction (OER) in photosynthesis,⁸⁴ water electrolysis,⁸⁵ hydrogen evolution reaction (HER),⁸⁶ hydrogen fuels cells,^{62,63} hydrodesulphurization,⁸⁷ synthesis of ammonia⁵⁶, CO₂ electro_reduction⁷² and Fischer–Tropsch process.⁵² Compositions with dominant AFM interactions are generally less active.

Milder adsorption energies and delocalized covalent bonds, both associated with spin-exchange hopping, make structures with predominant FM spin-polarized bonds consistently more noble-like. This is a key quantum “trick” that nature uses to evolve the most effective catalysts based on Earth-abundant metals (we would like to remind the reader at this point that QEXI in the

catalyst also play a role in the decrease of Coulomb repulsions, as seen in section 1.3. Then they should also intrinsically be included as an electronic factor that enhance activity).

Table 2 is an extension of Table 1; the energy terms of Table 2 differentiate the contribution of each spin (α or β) in open-shell configurations. We assume that α is the major spin population and, since $n_\alpha > n_\beta$, the number of $QSEI_{shell}^{open}$ versus the classical Coulomb terms is higher than in closed-shell systems. The meaning of the energy terms shown in Table 2 remains unchanged compared to the integrals in Table 1, albeit the electrons interact with each other and the modification of one potential affects the others. The additional spin energetic terms depending on $QSEI_{shells}^{open}$ comprise two possible spatial interactions, described in Table 3 and in Figure 7: the extra on-site $QSEI_{shells}^{open}$ interactions, taking place within the same atomic boundary (highlighted in dark blue in Figure 7) and the extra inter-atomic interactions, taking place among different atoms (orange in Figure 7) and only present in FM couplings.

Table 2. Most relevant quantum energy contributions related with energetic changes on magnetic catalysts.

$\Delta H_{cat.event}^{magnetic} = \Delta T_{e-}^{kinetic} + \Delta V_{N+e-}^{Coulomb} + \Delta V_{e-e-}^{Coulomb} + \Delta QSEI_{shells}^{open} + \Delta E_{e-}^{exc.corr.}$	
Energy Factor	Integral Expression
Kinetic energy spin- α	$T_{e-\alpha}^{kinetic} = \sum_a^{n_\alpha} \left\langle \psi_a^\alpha \left -\frac{1}{2} \nabla^2 \right \psi_a^\alpha \right\rangle$
Kinetic energy spin- β	$T_{e-\beta}^{kinetic} = \sum_{a'}^{n_\beta} \left\langle \psi_{a'}^\beta \left -\frac{1}{2} \nabla^2 \right \psi_{a'}^\beta \right\rangle$

<i>Coulomb nucleus-α attractions</i>	$\mathbf{V}_{N+e-\alpha}^{\text{Coulomb}} = - \sum_a^{n_\alpha} \sum_A^N \left\langle \psi_a^\alpha \left \frac{Z_A}{r_{1A}} \right \psi_a^\alpha \right\rangle$
<i>Coulomb nucleus-β attractions</i>	$\mathbf{V}_{N+e-\beta}^{\text{Coulomb}} = - \sum_{a'}^{n_\beta} \sum_A^N \left\langle \psi_{a'}^\beta \left \frac{Z_A}{r_{1A}} \right \psi_{a'}^\beta \right\rangle$
<i>Coulomb α-α repulsions</i>	$\mathbf{V}_{\alpha-\alpha}^{\text{Coulomb}} = \sum_a^{n_\alpha} \sum_{b>a}^{n_\alpha} \left\langle \psi_a^\alpha \psi_a^\alpha \left \frac{1}{r_{12}} \right \psi_a^\alpha \psi_a^\alpha \right\rangle$
<i>Coulomb β-β repulsions</i>	$\mathbf{V}_{\beta-\beta}^{\text{Coulomb}} = \sum_{a'}^{n_\beta} \sum_{b'>a'}^{n_\beta} \left\langle \psi_{a'}^\beta \psi_{b'}^\beta \left \frac{1}{r_{12}} \right \psi_{b'}^\beta \psi_{a'}^\beta \right\rangle$
<i>Coulomb α-β repulsions</i>	$\mathbf{V}_{\alpha-\beta}^{\text{Coulomb}} = \sum_a^{n_\alpha} \sum_{a'}^{n_\beta} \left\langle \psi_a^\alpha \psi_a^\alpha \left \frac{1}{r_{12}} \right \psi_{a'}^\beta \psi_{a'}^\beta \right\rangle$
<i>Quantum α-α exchange interaction</i>	$\mathbf{QSEI}_{\alpha-\alpha} = - \sum_a^{n_\alpha} \sum_{b>a}^{n_\alpha} \left\langle \psi_a^\alpha \psi_b^\alpha \left \frac{1}{r_{12}} \right \psi_b^\alpha \psi_a^\alpha \right\rangle$
<i>Quantum β-β exchange interaction</i>	$\mathbf{QSEI}_{\beta-\beta} = - \sum_{a'}^{n_\beta} \sum_{b'>a'}^{n_\beta} \left\langle \psi_{a'}^\beta \psi_{b'}^\beta \left \frac{1}{r_{12}} \right \psi_{b'}^\beta \psi_{a'}^\beta \right\rangle$
<i>Quantum Excitation Correlation</i>	$\mathbf{QEXI} = \mathbf{E}_{e-}^{\text{exc.corr.}}$

Table 3. On-site and inter-atomic $QSEI_{shell}^{open}$ for the extra $\alpha(\beta)$ -spins in magnetic catalysts.

$QSEI_{\alpha-\alpha} = QSEI_{on-site}^{A-A} + QSEI_{inter-atomic}^{FM.A-B}$	
Energy Factor	Integral Expression
<i>A-A on-site Exchange Interaction</i>	$\sum_A^N \sum_a^{A_\alpha} \sum_{b>a}^{e-\alpha_A} \left\langle \psi_{a-A}^\alpha \psi_{b-A}^\alpha \left \frac{1}{r_{12}} \right \psi_{b-A}^\alpha \psi_{a-A}^\alpha \right\rangle$
<i>FM A-B inter-atomic Exchange Interaction</i>	$\sum_A^N \sum_{B>A}^N \sum_a^{e-\alpha_A} \sum_b^{e-\alpha_B} \left\langle \psi_{a-A}^\alpha \psi_{b-B}^\alpha \left \frac{1}{r_{12}} \right \psi_{b-B}^\alpha \psi_{a-A}^\alpha \right\rangle$

Strong intra-atomic QSEI localize in space within the $3d-4f$ open shells in systems with dominant AFM couplings, Figure 7 left; $QSEI_{on-site}^{A-A}$ allow very stable high-spin orbital configurations by reducing exclusively the on-site electronic repulsions. There are no extra inter-atomic $QSEI_{shells}^{open}$ (orange terms in Figure 7) between AFM-coupled spin-configurations; the inter-atomic Coulomb repulsions are intact in the catalyst, thus typically, AFM Jahn-Teller (J.-T.) elongations emerge to help reducing the electronic repulsions. J.-T. AFM distortions might appear along the direction of the highest occupied anti-bonding orbitals.⁸⁵

Two electronic factors tend to reduce the catalytic activity in materials based on $3d$ -metals with predominant AFM orderings: a) the stabilization and additional localization of the electron pairs, Fermi heaps, between metal centers and b) the relative destabilization of the lowest unoccupied orbitals. This fact is likewise related with the enhanced electronic localization in space as Figure 8 (center) shows. In the excellent work by Landrum and Dronskowski in 2000,⁷³ the authors report a reduced number of states at the Fermi level for AFM Cr and Mn; they explain that magnetic interactions reduce the radial extension of the $3d$ -orbitals. This is an understandable phenomenon

in quantum mechanics because exchange interactions, as we describe, reduce the electronic repulsions. The catalytic activity drops especially for AFM Mott insulators, with the opening of a band gap between the occupied Mott lower valence band and the empty upper conduction band. For instance, $3d^3\text{-Cr}^{3+}$ (e.g., LaCrO_3) and $3d^5\text{-Fe}^{3+}$ (e.g., LaFeO_3) AFM insulators are among the worst compositions in oxygen catalysis. Once a robust fully AFM configuration is assembled, whether including or not the ligands/intermediates, any possible alteration proves to be difficult because: a) the strongly correlated electrons are stabilized via on-site $\text{QSEI}_{shell}^{open}$ and J.-T. distortions and b) the magnetically fully occupied high-spin $3d^3$ or $3d^5$ orbital configurations will repel possible incoming electron density. For HER, ΔH_{ads}^{H*} is endothermic for Cr and Mn metals because the term $\Delta V_{e-e}^{Coulomb} > 0$ weakens the interaction between the catalyst and the reactant.

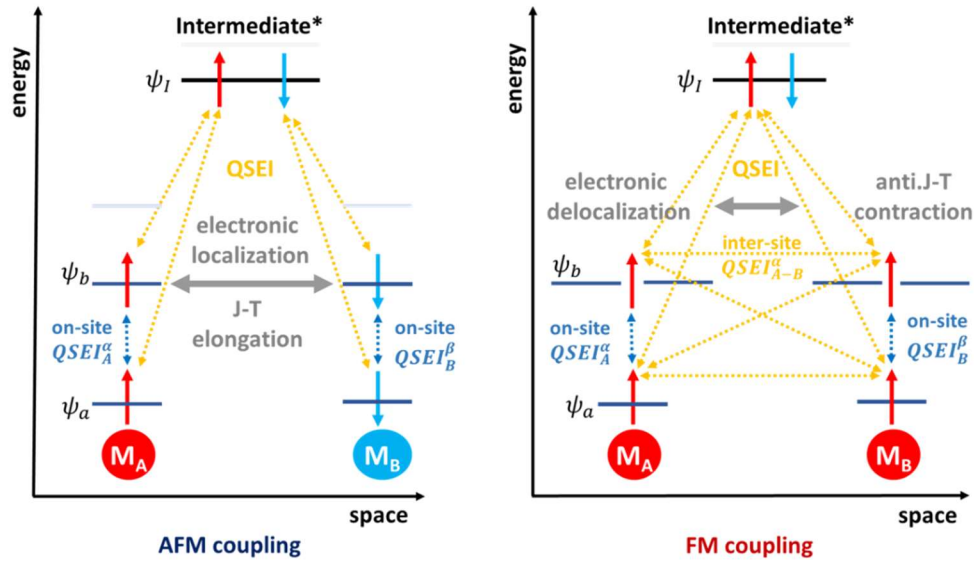


Figure 7. Simplified $\text{QSEI}_{shell}^{open}$ energy/space plots for catalysts with predominant AFM (left) or FM (right) couplings. The dark-blue dotted arrows indicate the on-site $\text{QSEI}_{shell}^{open}$, while the orange ones show the inter-atomic QSEI.

In FM bonds, Figure 7 right, the total number of electrons with spin- α (n_α) is different than the number of electrons with spin- β (n_β) and, since $n_\alpha^{FM} > n_\beta^{FM}$, growing the amount of inter-atomic QSEI_{shell}^{open} centers on the valence band creating Fermi holes that increase the exchange spin-delocalization and decreasing the electronic repulsions. Strongly correlated itinerant electrons in FM domains have a profound impact in catalysis and they add spin-polarization to the thermodynamics. Bhattacharjee and Lee observed spin-polarized oxygen atoms adsorbed on the FM PdFe alloy and controlled oxygen reduction through the spin orientation.⁶¹ The same authors reported a non-linear trend in NH₃ adsorption energy on FM metals.²³ These observations lead Bhattacharjee and Lee to reformulate the d-band model to try to take partially into account the catalytic activity of spin-polarized materials.⁵⁹ This proposed approach improves the electronic description, but the approach still lacks of a full quantum correlated theory.

Notice that the QSEI space-time mechanism in Figure 1 left is more recurrent and crucially important in a material having a dominant FM ground state, Figure 7 right. Electrons with the same spin can exchange their orbitals more frequently, their electronic repulsions decrease inside the catalysts and such additional stabilizing energy together with empty valence orbitals yields to enhanced catalytic activity via pure quantum interactions.

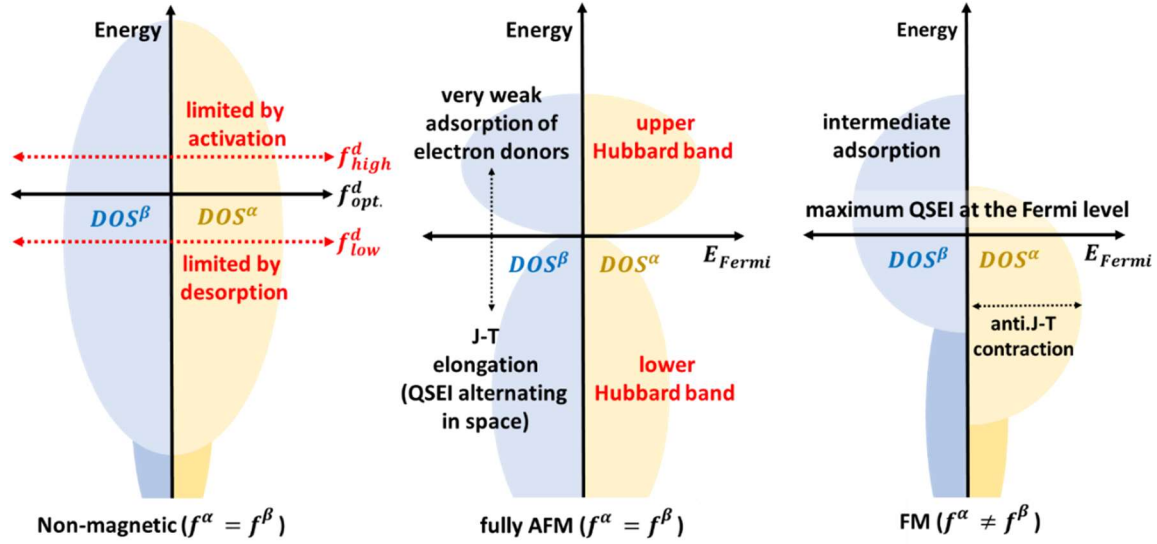


Figure 8. Sketched changes for the density of states (DOS) for non-magnetic (left), predominant antiferromagnetic (center) and predominant ferromagnetic compositions (right).

Figure 8 shows that $QSEI_{shell}^{open}$ can have a profound impact on the shape and energy of the electronic states. The density of states (DOS) is symmetric for both non-magnetic (closed shell, Figure 8 left) and fully AFM materials (Figure 8 center). The difference between the former and the latter spin configurations lies in two essential aspects: the full delocalization of the QSEI in space and energy for closed-shell materials; on the other hand, the dropping in energy of the occupied shells (lower Hubbard band) and raising in energy of the empty levels (upper Hubbard band) for materials with dominant AFM interactions.⁵⁹ The inter-atomic Coulomb attractions dominate and help in the stabilization of electron pairs in AFM bonds (Mottness). Extending the concepts developed by Goodenough,⁸⁸ compositions with half-filled bands (at their own oxidations

states and crystal field) show predominant AFM couplings. In this case, the intra-atomic $QSEI_{shells}^{open}$ can make the catalyst more inert, resembling d^{l0} configurations.

The orbital degeneracies accumulate at the valence band for FM orderings. $QSEI_{shells}^{open}$ make the strongly correlated itinerant unpaired electrons collectively more stable at the Fermi level causing, for instance, the almost similar HER activity seen for Fe, Co and Ni metals.⁸⁹ FM $QSEI_{shells}^{open}$ yield to moderate binding energies, spin-selectivity, and enhanced redox transfers during catalytic reactions at the covalent active sites. For instance, FM conducting structures based on electron-rich magnetic metals (like $Mn^{\sim 3.25+}$, $Fe^{\sim 3.25+}$ and $Co^{\sim 3.25+}$ oxides) may become excellent oxygen reduction catalysts,^{63,34} while configurations with fewer electrons ($Mn^{\sim 3.75+}$ or $Co^{\sim 3.75+}$ oxides) are particularly suitable to accelerate oxygen evolution.^{2,1}

2.3 Quantifying catalytic trends in strongly correlated magnetic systems.

Eq. 2 has been deduced by the authors as a simple and quite straightforward modification of Eq. 1⁸⁵ when either dominant FM or AFM orderings are present in the catalytic structure. $\vec{S}_{cat.}$ is the magnetic moment accumulated at the crucial bonds-atoms; if $\vec{S}_{cat.} = \mathbf{0}$, we are in the classical parabolic regime versus f_d .

$$\text{Eq. 2) } \Delta H_{activation}^{(non-)\text{magnetic}} = a(f_d - h)^2 + k \pm \Delta J_{activation}^{QSEI_{shells}^{open}}(f_d) \cdot \vec{S}_{cat.}(f_d)$$

When $\vec{S}_{cat.}(f_d) > 0$, the on-site $QSEI_{shells}^{open}$ stabilize the d-orbitals reducing the adsorption energies, see Figure 7. For those processes limited by the desorption of the reactants (h is typically too high on metals exception made for d^{10} configurations) the activity increases because of the term $-\Delta J_{activation}^{QSEI_{shells}^{open}}(f_d) \cdot \vec{S}_{cat.}(f_d)$. FM $QSEI_{shells}^{open}$ make the catalysts behave as more “noble” (compared with one of the same f_d , but without ferromagnetic QSEI) and this is usually an energetic advantage to enhance reaction rates using abundant magnetic metals. However, in presence of major inter-atomic AFM $QSEI_{shells}^{open}$, the additional localization of electron pairs^{1,2} yields usually to higher activation barriers (i.e., the activity decreases), because of limited ionic and electronic mobility and very weak adsorption of electron donors, hence $+\Delta J_{activation}^{QSEI_{shells}^{open}}(f_d) \cdot \vec{S}_{cat.}(f_d)$. The terms $\Delta J_{activation}^{QSEI_{shells}^{open}}(f_d)$ and $\vec{S}_{cat.}(f_d)$ may be determined from experiments at the actual reaction conditions and provide the basic theoretical foundation to understand multi-peak trends versus f_d ,^{38,1,90} Figure 9.

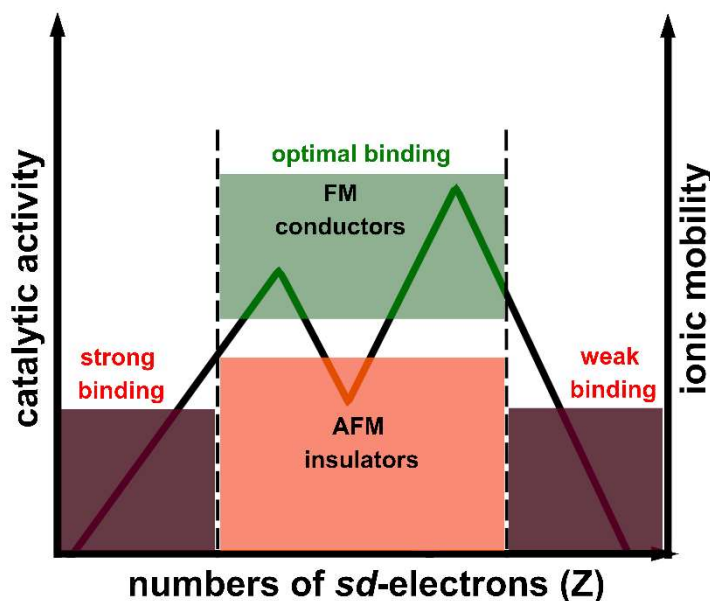


Figure 9. Schematic multi-peak activity trend for catalysts based on 3d-metals for similar coordination and oxidation states. The activity is plotted versus the oscillation of their magnetic properties due to changes in the orbital filling.

3. Conclusions

Strongly correlated electrons have drastic effects on the energy of magnetic materials in catalysis. Just as spintronics deals with advanced spin-based technology and devices where both the charge and spin of the electrons are modulated to offer a wide diversity of functionalities,⁹¹ similarly, the idea that the surface reactivity may be modulated by the influence of cooperative spin-potentials $\text{QSEI}_{\text{shells}}^{\text{open}}$ via the orbital engineering of earth-abundant magnetic systems is a tangible reality. Strongly correlated electrons, in fact, can affect the efficiency, cost, implementation and environmental footprint of any heterogeneous catalyst. Quantum spin exchange interactions, QSEI and QEXI, are a subtle phenomenon lying outside of the domain of classical physics, but their presence is effectively responsible for the unusual intrinsic properties of magnetic catalysts. The influence of cooperative $\text{QSEI}_{\text{shell}}^{\text{open}}$ in materials with unpaired-electrons can be seen in their

characteristic structure, electronic conductivity, chemical bonding, catalytic activity and selectivity.

We have mainly presented the physics that describe and rationalize the quantummechanic origin of $\text{QSEI}_{\text{shell}}^{\text{open}}$, showing how diverse cooperative $\text{QSEI}_{\text{shell}}^{\text{open}}$ alter electronic transfer steps between adsorbates and magnetic catalysts. This improved theoretical description is the only path to understand strongly correlated catalysts. A complete treatment of orbital physics, synergistically integrated into classical catalytic concepts like the Sabatier's principle, d-band theory or volcano plots promises to improve predictions in the design of future catalysts and technologies.

The general take-home message for experimentalists attempting to gain knowledge on how to design catalysts with improved activity is: ferro- or ferri- magnetic catalysts are always preferred over non-magnetic or antiferromagnetic catalysts (the most useful antiferromagnetism is the layered one, as in AFM type-A), control as accurately as possible the size and the layering of your particles (e.g., magnetic catalysts in thin films are preferable, in our opinion, for the ability to tune more appropriately the magnetization inside those films), induce the presence of defects studying their impact on the catalysis, including magnetic supports (as in the case of nitrogen-doped graphene).

AUTHOR INFORMATION

Corresponding Author

*Jose Gracia, ORCID: 0000-0001-7744-8872

E-mail: jose.gracia@magnetocat.com

Authors

Chiara Biz, ORCID: 0000-0003-3104-552X

Mauro Fianchini, ORCID: 0000-0003-2619-7932

Author Contributions

The manuscript was written through contributions of all authors.

Notes

The authors declare no conflict of interest.

ACKNOWLEDGMENT

This project has received funding from the European Union's Horizon 2020 research and innovation programme under grant agreement No. 964972 (H2020-FETOPEN-2018-2019-2020-01). CB, MF and JG thank the SpinCat consortium and the Ministerio de Ciencia e Innovación (España) to recognize MagnetoCat SL as "Pyme Innovadora".

REFERENCES

- (1) Gracia, J.; Sharpe, R.; Munarriz, J. *Principles Determining the Activity of Magnetic Oxides for Electron Transfer Reactions*. *J. Catal.* **2018**, *361*, 331–338. <https://doi.org/10.1016/j.jcat.2018.03.012>.
- (2) Gracia, J. *Spin Dependent Interactions Catalyse the Oxygen Electrochemistry*. *Phys. Chem. Chem. Phys.* **2017**, *19* (31), 20451–20456. <https://doi.org/10.1039/C7CP04289B>.
- (3) Gracia, J. *What Are the Electrons Really Doing in Molecules? A Space-Time Picture*. *Eur. J. Phys. Educ. Vol 11 No 1* **2020**.
- (4) Dirac, P. A. M. *The Lagrangian in Quantum Mechanics*. *Phys. Zeits. Sowjetunion* **1933**, *3*, 64–72.
- (5) Einstein, A. *Ist Die Trägheit Eines Körpers von Seinem Energieinhalt Abhängig?* *Ann. Phys.* **1905**, *323* (13), 639–641. <https://doi.org/10.1002/andp.19053231314>.
- (6) Einstein, A. *Ist Die Trägheit Eines Körpers von Seinem Energieinhalt Abhängig?* [*AdP 18, 639 (1905)*]. *Ann. Phys.* **2005**, *14* (AdP 18, 639 (1905)), 225–228. <https://doi.org/10.1002/andp.200590007>.

- (7) Szabo, A.; Ostlund, N. *Modern Quantum Chemistry : Introduction to Advanced Electronic Structure Theory* / Attila Szabo, Neil S. Ostlund; 2018.
- (8) Ren, X.; Wu, T.; Sun, Y.; Li, Y.; Xian, G.; Liu, X.; Shen, C.; Gracia, J.; Gao, H.-J.; Yang, H.; Xu, Z. J. *Spin-Polarized Oxygen Evolution Reaction under Magnetic Field*. *Nat. Commun.* **2021**, 12 (1), 2608. <https://doi.org/10.1038/s41467-021-22865-y>.
- (9) Caruso, F.; Rohr, D. R.; Hellgren, M.; Ren, X.; Rinke, P.; Rubio, A.; Scheffler, M. *Bond Breaking and Bond Formation: How Electron Correlation Is Captured in Many-Body Perturbation Theory and Density-Functional Theory*. *Phys. Rev. Lett.* **2013**, 110 (14), 146403. <https://doi.org/10.1103/PhysRevLett.110.146403>.
- (10) Sherrill, C. D.; Dutta, A.; Abrams, M. L.; Sears, J. S. *Bond Breaking in Quantum Chemistry: A Comparison of Single- and Multi-Reference Methods*; 2007; pp 75–88. <https://doi.org/10.1021/bk-2007-0958.ch005>.
- (11) Goodenough, J. B. *Localized-Itinerant Electronic Transitions in Oxides and Sulfides*. *J. Alloys Compd.* **1997**, 262–263 (I), 1–9. [https://doi.org/10.1016/S0925-8388\(97\)00321-6](https://doi.org/10.1016/S0925-8388(97)00321-6).
- (12) Garcés-Pineda, F. A.; Blasco-Ahicart, M.; Nieto-Castro, D.; López, N.; Galán-Mascarós, J. R. *Direct Magnetic Enhancement of Electrocatalytic Water Oxidation in Alkaline Media*. *Nat. Energy* **2019**, 4 (6), 519–525. <https://doi.org/10.1038/s41560-019-0404-4>.
- (13) Mtangi, W.; Tassinari, F.; Vankayala, K.; Vargas Jentzsch, A.; Adelizzi, B.; Palmans, A. R. A.; Fontanesi, C.; Meijer, E. W.; Naaman, R. *Control of Electrons' Spin Eliminates Hydrogen Peroxide Formation During Water Splitting*. *J. Am. Chem. Soc.* **2017**, 139 (7), 2794–2798. <https://doi.org/10.1021/jacs.6b12971>.
- (14) Ghosh, S.; Bloom, B. P.; Lu, Y.; Lamont, D.; Waldeck, D. H. *Increasing the Efficiency of Water Splitting through Spin Polarization Using Cobalt Oxide Thin Film Catalysts*. *J. Phys. Chem. C* **2020**, 124 (41), 22610–22618. <https://doi.org/10.1021/acs.jpcc.0c07372>.
- (15) Ghosh, S.; Bloom, B. P.; Lu, Y.; Lamont, D.; Waldeck, D. H. *Increasing the Efficiency of Water Splitting through Spin Polarization Using Cobalt Oxide Thin Film Catalysts*. *J. Phys. Chem. C* **2020**, 124 (41), 22610–22618. <https://doi.org/10.1021/acs.jpcc.0c07372>.
- (16) Wu, T.; Ren, X.; Sun, Y.; Sun, S.; Xian, G.; Scherer, G. G.; Fisher, A. C.; Mandler, D.; Ager, J. W.; Grimaud, A.; Wang, J.; Shen, C.; Yang, H.; Gracia, J.; Gao, H.-J.; Xu, Z. J. *Spin Pinning Effect to Reconstructed Oxyhydroxide Layer on Ferromagnetic Oxides for Enhanced Water Oxidation*. *Nat. Commun.* **2021**, 12 (1), 3634. <https://doi.org/10.1038/s41467-021-23896-1>.
- (17) Zeng, J.; Liao, S.; Lee, J. Y.; Liang, Z. *Oxygen Reduction Reaction Operated on Magnetically-Modified PtFe/C Electrocatalyst*. *Int. J. Hydrogen Energy* **2010**, 35 (3), 942–948. <https://doi.org/10.1016/j.ijhydene.2009.11.055>.
- (18) Garg, N.; Mishra, M.; Govind; Ganguli, A. K. *Electrochemical and Magnetic Properties of Nanostructured CoMn₂O₄ and Co₂MnO₄*. *RSC Adv.* **2015**, 5 (103), 84988–84998. <https://doi.org/10.1039/C5RA16937B>.

- (19) Zhou, W.; Chen, M.; Guo, M.; Hong, A.; Yu, T.; Luo, X.; Yuan, C.; Lei, W.; Wang, S. *Magnetic Enhancement for Hydrogen Evolution Reaction on Ferromagnetic MoS₂ Catalyst*. *Nano Lett.* **2020**, *20* (4), 2923–2930. <https://doi.org/10.1021/acs.nanolett.0c00845>.
- (20) Zhang, Y.; Liang, C.; Wu, J.; Liu, H.; Zhang, B.; Jiang, Z.; Li, S.; Xu, P. *Recent Advances in Magnetic Field-Enhanced Electrocatalysis*. *ACS Appl. Energy Mater.* **2020**, *3* (11), 10303–10316. <https://doi.org/10.1021/acsaem.0c02104>.
- (21) Spatzal, T.; Einsle, O.; Andrade, S. L. A. *Analysis of the Magnetic Properties of Nitrogenase FeMo Cofactor by Single-Crystal EPR Spectroscopy*. *Angew. Chemie Int. Ed.* **2013**, *52* (38), 10116–10119. <https://doi.org/10.1002/anie.201303000>.
- (22) Hughes, J. P.; Rowley-Neale, S.; Banks, C. *Enhancing the Efficiency of the Hydrogen Evolution Reaction Utilising Fe₃P Bulk Modified Screen-Printed Electrodes via the Application of a Magnetic Field*. *RSC Adv.* **2021**, *11* (14), 8073–8079. <https://doi.org/10.1039/D0RA10150H>.
- (23) Bhattacharjee, S.; Yoo, S. J.; Waghmare, U. V.; Lee, S. C. *NH₃ Adsorption on PtM (Fe, Co, Ni) Surfaces: Cooperating Effects of Charge Transfer, Magnetic Ordering and Lattice Strain*. *Chem. Phys. Lett.* **2016**, *648*, 166–169. <https://doi.org/10.1016/j.cplett.2016.01.031>.
- (24) Li, Y.; Zhang, L.; Peng, J.; Zhang, W.; Peng, K. *Magnetic Field Enhancing Electrocatalysis of Co₃O₄/NF for Oxygen Evolution Reaction*. *J. Power Sources* **2019**, *433*, 226704. <https://doi.org/10.1016/j.jpowsour.2019.226704>.
- (25) Yang, Q.; Du, J.; Nie, X.; Yang, D.; Bian, L.; Yang, L.; Dong, F.; He, H.; Zhou, Y.; Yang, H. *Magnetic Field-Assisted Photoelectrochemical Water Splitting: The Photoelectrodes Have Weaker Nonradiative Recombination of Carrier*. *ACS Catal.* **2021**, *11* (3), 1242–1247. <https://doi.org/10.1021/acscatal.0c05436>.
- (26) Pecchi, G.; Campos, C.; Peña, O.; Cadus, L. E. *Structural, Magnetic and Catalytic Properties of Perovskite-Type Mixed Oxides LaMn_{1-y}Co_yO₃ (y = 0.0, 0.1, 0.3, 0.5, 0.7, 0.9, 1.0)*. *J. Mol. Catal. A Chem.* **2008**, *282* (1–2), 158–166. <https://doi.org/10.1016/j.molcata.2007.12.022>.
- (27) Li, Z.; Lv, Z.; Liu, X.; Wang, G.; Lin, Y.; Xie, G.; Jiang, L. *Magnetic-Field Guided Synthesis of Highly Active Ni–S–CoFe₂O₄ Electrocatalysts for Oxygen Evolution Reaction*. *Renew. Energy* **2021**, *165*, 612–618. <https://doi.org/10.1016/j.renene.2020.11.083>.
- (28) Zhao, Z.; Wang, D.; Gao, R.; Wen, G.; Feng, M.; Song, G.; Zhu, J.; Luo, D.; Tan, H.; Ge, X.; Zhang, W.; Zhang, Y.; Zheng, L.; Li, H.; Chen, Z. *Magnetic-Field-Stimulated Efficient Photocatalytic N₂ Fixation over Defective BaTiO₃ Perovskites*. *Angew. Chemie Int. Ed.* **2021**, anie.202100726. <https://doi.org/10.1002/anie.202100726>.
- (29) Dagotto, E. *Complexity in Strongly Correlated Electronic Systems*. *Science* (80-.). **2005**, *309* (5732), 257–262. <https://doi.org/10.1126/science.1107559>.
- (30) Fletcher, S. *The Theory of Electron Transfer*. *J. Solid State Electrochem.* **2010**, *14* (5), 705–

739. <https://doi.org/10.1007/s10008-009-0994-z>.
- (31) Fletcher, S.; Van Dijk, N. J. *Supercatalysis by Superexchange*. *J. Phys. Chem. C* **2016**, *120* (46), 26225–26234. <https://doi.org/10.1021/acs.jpcc.6b09099>.
 - (32) Dagotto, E.; Tokura, Y. *Strongly Correlated Electronic Materials: Present and Future*. *MRS Bull.* **2008**, *33* (11), 1037–1045. <https://doi.org/10.1557/mrs2008.223>.
 - (33) Goodenough, J. B. *An Interpretation of the Magnetic Properties of the Perovskite-Type Mixed Crystals $\text{La}_{1-x}\text{Sr}_x\text{CoO}_3-\lambda$* . *J. Phys. Chem. Solids* **1958**, *6* (2–3), 287–297. [https://doi.org/10.1016/0022-3697\(58\)90107-0](https://doi.org/10.1016/0022-3697(58)90107-0).
 - (34) Sharpe, R.; Munarriz, J.; Lim, T.; Jiao, Y.; Niemantsverdriet, J. W.; Polo, V.; Gracia, J. *Orbital Physics of Perovskites for the Oxygen Evolution Reaction*. *Top. Catal.* **2018**, *61* (3–4), 267–275. <https://doi.org/10.1007/s11244-018-0895-4>.
 - (35) Goodenough, J. .; Zhou, J.-S.; Rivadulla, F.; Winkler, E. *Bond-Length Fluctuations in Transition-Metal Oxoperovskites*. *J. Solid State Chem.* **2003**, *175* (1), 116–123. [https://doi.org/10.1016/S0022-4596\(03\)00041-0](https://doi.org/10.1016/S0022-4596(03)00041-0).
 - (36) Goodenough, J. B. *JAHN-TELLER PHENOMENA IN SOLIDS*. *Annu. Rev. Mater. Sci.* **1998**, *28* (1), 1–27. <https://doi.org/10.1146/annurev.matsci.28.1.1>.
 - (37) Goodenough, J. B. *Localized-Itinerant Electronic Transitions in Oxides and Sulfides*. *J. Alloys Compd.* **1997**, *262–263* (I), 1–9. [https://doi.org/10.1016/S0925-8388\(97\)00321-6](https://doi.org/10.1016/S0925-8388(97)00321-6).
 - (38) Jiao, Y.; Sharpe, R.; Lim, T.; Niemantsverdriet, J. W. H.; Gracia, J. *Photosystem II Acts as a Spin-Controlled Electron Gate during Oxygen Formation and Evolution*. *J. Am. Chem. Soc.* **2017**, *139* (46), 16604–16608. <https://doi.org/10.1021/jacs.7b07634>.
 - (39) Williams, R. J. P. *Metallo-Enzyme Catalysis*. *Chem. Commun.* **2003**, *3* (10), 1109–1113. <https://doi.org/10.1039/b211281g>.
 - (40) Zhang, H.; Li, S.; Qu, A.; Hao, C.; Sun, M.; Xu, L.; Xu, C.; Kuang, H. *Engineering of Chiral Nanomaterials for Biomimetic Catalysis*. *Chem. Sci.* **2020**, *11* (48), 12937–12954. <https://doi.org/10.1039/D0SC03245J>.
 - (41) Ageeva, A.; Khramtsova, E.; Magin, I.; Polyakov, N.; Miranda, M.; Leshina, T. *Peculiarities of Electron Transfer in Chiral Linked Systems*. In *Chirality from Molecular Electronic States*; IntechOpen, 2019. <https://doi.org/10.5772/intechopen.82684>.
 - (42) Kumar, A.; Capua, E.; Kesharwani, M. K.; Martin, J. M. L.; Sitbon, E.; Waldeck, D. H.; Naaman, R. *Chirality-Induced Spin Polarization Places Symmetry Constraints on Biomolecular Interactions*. *Proc. Natl. Acad. Sci.* **2017**, *114* (10), 2474–2478. <https://doi.org/10.1073/pnas.1611467114>.
 - (43) Mondal, P. C.; Fontanesi, C.; Waldeck, D. H.; Naaman, R. *Spin-Dependent Transport through Chiral Molecules Studied by Spin-Dependent Electrochemistry*. *Acc. Chem. Res.* **2016**, *49* (11), 2560–2568. <https://doi.org/10.1021/acs.accounts.6b00446>.

- (44) Naaman, R.; Paltiel, Y.; Waldeck, D. H. *Chiral Molecules and the Electron Spin*. *Nat. Rev. Chem.* **2019**, 3 (4), 250–260. <https://doi.org/10.1038/s41570-019-0087-1>.
- (45) Marx-Tibbon, S.; Katz, E.; Willner, I. *Chiral Recognition in Mediated Electron Transfer in Redox Proteins*. *J. Am. Chem. Soc.* **1995**, 117 (39), 9925–9926. <https://doi.org/10.1021/ja00144a025>.
- (46) Trasatti, S. Electrocatalysis of Hydrogen Evolution: Progress in Cathode Activation. In *Advances in Electrochemical Science and Engineering*; 1991; Vol. 2, pp 1–85. <https://doi.org/10.1002/9783527616763.ch1>.
- (47) Greeley, J.; Jaramillo, T. F.; Bonde, J.; Chorkendorff, I.; Nørskov, J. K. *Computational High-Throughput Screening of Electrocatalytic Materials for Hydrogen Evolution*. *Nat. Mater.* **2006**, 5 (11), 909–913. <https://doi.org/10.1038/nmat1752>.
- (48) Kremeníć, G.; Nieto, J. M. L.; Tascón, J. M. D.; Tejuca, L. G. *Chemisorption and Catalysis on LaMO₃ Oxides*. *J. Chem. Soc. Faraday Trans. 1 Phys. Chem. Condens. Phases* **1985**, 81 (4), 939. <https://doi.org/10.1039/f19858100939>.
- (49) Hong, W. T.; Welsch, R. E.; Shao-Horn, Y. *Descriptors of Oxygen-Evolution Activity for Oxides: A Statistical Evaluation*. *J. Phys. Chem. C* **2016**, 120 (1), 78–86. <https://doi.org/10.1021/acs.jpcc.5b10071>.
- (50) Han, B.; Risch, M.; Lee, Y.-L.; Ling, C.; Jia, H.; Shao-Horn, Y. *Activity and Stability Trends of Perovskite Oxides for Oxygen Evolution Catalysis at Neutral PH*. *Phys. Chem. Chem. Phys.* **2015**, 17 (35), 22576–22580. <https://doi.org/10.1039/C5CP04248H>.
- (51) Kojima, T.; Kameoka, S.; Tsai, A.-P. *The Emergence of Heusler Alloy Catalysts*. *Sci. Technol. Adv. Mater.* **2019**, 20 (1), 445–455. <https://doi.org/10.1080/14686996.2019.1598238>.
- (52) Gracia, J. M.; Prinsloo, F. F.; Niemantsverdriet, J. W. *Mars-van Krevelen-like Mechanism of CO Hydrogenation on an Iron Carbide Surface*. *Catal. Letters* **2009**, 133 (3–4), 257–261. <https://doi.org/10.1007/s10562-009-0179-5>.
- (53) Kremeníć, G.; Nieto, J. M. L.; Tascón, J. M. D.; Tejuca, L. G. *Chemisorption and Catalysis on LaMO₃ Oxides*. *J. Chem. Soc. Faraday Trans. 1 Phys. Chem. Condens. Phases* **1985**, 81 (4), 939. <https://doi.org/10.1039/f19858100939>.
- (54) Hong, W. T.; Welsch, R. E.; Shao-Horn, Y. *Descriptors of Oxygen-Evolution Activity for Oxides: A Statistical Evaluation*. *J. Phys. Chem. C* **2016**, 120 (1), 78–86. <https://doi.org/10.1021/acs.jpcc.5b10071>.
- (55) PECORARO, T. *Hydrodesulfurization Catalysis by Transition Metal Sulfides*. *J. Catal.* **1981**, 67 (2), 430–445. [https://doi.org/10.1016/0021-9517\(81\)90303-1](https://doi.org/10.1016/0021-9517(81)90303-1).
- (56) Munarriz, J.; Polo, V.; Gracia, J. *On the Role of Ferromagnetic Interactions in Highly Active Mo-Based Catalysts for Ammonia Synthesis*. *ChemPhysChem* **2018**, 19 (21), 2843–2847. <https://doi.org/10.1002/cphc.201800633>.

- (57) Nazmutdinov, R. R.; Santos, E.; Schmickler, W. *Spin Effects in Oxygen Electrocatalysis: A Discussion. Electrochem. commun.* **2013**, *33*, 14–17. <https://doi.org/10.1016/j.elecom.2013.04.001>.
- (58) Choudhary, R.; Manchanda, P.; Enders, A.; Balamurugan, B.; Kashyap, A.; Sellmyer, D. J.; Sykes, E. C. H.; Skomski, R. *Spin-Modified Catalysis. J. Appl. Phys.* **2015**, *117* (17), 17D720. <https://doi.org/10.1063/1.4917328>.
- (59) Bhattacharjee, S.; Waghmare, U. V.; Lee, S.-C. *An Improved D-Band Model of the Catalytic Activity of Magnetic Transition Metal Surfaces. Sci. Rep.* **2016**, *6* (1), 35916. <https://doi.org/10.1038/srep35916>.
- (60) Escaño, M. C. S.; Kasai, H. *A Novel Mechanism of Spin-Orientation Dependence of O₂ Reactivity from First Principles Methods. Catal. Sci. Technol.* **2017**, *7* (5), 1040–1044. <https://doi.org/10.1039/C6CY01198E>.
- (61) Bhattacharjee, S.; Lee, S.-C. *Controlling Oxygen-Based Electrochemical Reactions through Spin Orientation. J. Phys. Chem. C* **2018**, *122* (1), 894–901. <https://doi.org/10.1021/acs.jpcc.7b10147>.
- (62) Biz, C.; Fianchini, M.; Polo, V.; Gracia, J. *Magnetism and Heterogeneous Catalysis: In Depth on the Quantum Spin-Exchange Interactions in Pt 3 M (M = V, Cr, Mn, Fe, Co, Ni, and Y)(111) Alloys. ACS Appl. Mater. Interfaces* **2020**, *12* (45), 50484–50494. <https://doi.org/10.1021/acsami.0c15353>.
- (63) Biz, C.; Fianchini, M.; Gracia, J. *Catalysis Meets Spintronics; Spin Potentials Associated with Open-Shell Orbital Configurations Enhance the Activity of Pt 3 Co Nanostructures for Oxygen Reduction: A Density Functional Theory Study. ACS Appl. Nano Mater.* **2020**, *3* (1), 506–515. <https://doi.org/10.1021/acsanm.9b02067>.
- (64) Hong, W. T.; Gadre, M.; Lee, Y.-L.; Biegalski, M. D.; Christen, H. M.; Morgan, D.; Shao-Horn, Y. *Tuning the Spin State in LaCoO₃ Thin Films for Enhanced High-Temperature Oxygen Electrocatalysis. J. Phys. Chem. Lett.* **2013**, *4* (15), 2493–2499. <https://doi.org/10.1021/jz401271m>.
- (65) Liu, Y.; Xiao, C.; Lyu, M.; Lin, Y.; Cai, W.; Huang, P.; Tong, W.; Zou, Y.; Xie, Y. *Ultrathin Co₃S₄ Nanosheets That Synergistically Engineer Spin States and Exposed Polyhedra That Promote Water Oxidation under Neutral Conditions. Angew. Chemie Int. Ed.* **2015**, *54* (38), 11231–11235. <https://doi.org/10.1002/anie.201505320>.
- (66) Ramsundar, R. M.; Pillai, V. K.; Joy, P. A. *Spin State Engineered Zn_xCo_{3-x}O₄ as an Efficient Oxygen Evolution Electrocatalyst. Phys. Chem. Chem. Phys.* **2018**, *20* (46), 29452–29461. <https://doi.org/10.1039/C8CP06641H>.
- (67) Zhou, S.; Miao, X.; Zhao, X.; Ma, C.; Qiu, Y.; Hu, Z.; Zhao, J.; Shi, L.; Zeng, J. *Engineering Electrocatalytic Activity in Nanosized Perovskite Cobaltite through Surface Spin-State Transition. Nat. Commun.* **2016**, *7* (1), 11510. <https://doi.org/10.1038/ncomms11510>.
- (68) Lim, T.; Niemantsverdriet, J. W. H.; Gracia, J. *Layered Antiferromagnetic Ordering in the*

- Most Active Perovskite Catalysts for the Oxygen Evolution Reaction. ChemCatChem* **2016**, 8 (18), 2968–2974. <https://doi.org/10.1002/cctc.201600611>.
- (69) Sharpe, R.; Lim, T.; Jiao, Y.; Niemantsverdriet, J. W. H.; Gracia, J. *Oxygen Evolution Reaction on Perovskite Electrocatalysts with Localized Spins and Orbital Rotation Symmetry. ChemCatChem* **2016**, 8 (24), 3762–3768. <https://doi.org/10.1002/cctc.201600835>.
- (70) Pan, L.; Ai, M.; Huang, C.; Yin, L.; Liu, X.; Zhang, R.; Wang, S.; Jiang, Z.; Zhang, X.; Zou, J.-J.; Mi, W. *Manipulating Spin Polarization of Titanium Dioxide for Efficient Photocatalysis. Nat. Commun.* **2020**, 11 (1), 418. <https://doi.org/10.1038/s41467-020-14333-w>.
- (71) Chen, R. R.; Sun, Y.; Ong, S. J. H.; Xi, S.; Du, Y.; Liu, C.; Lev, O.; Xu, Z. J. *Antiferromagnetic Inverse Spinel Oxide LiCoVO₄ with Spin-Polarized Channels for Water Oxidation. Adv. Mater.* **2020**, 32 (10), 1907976. <https://doi.org/10.1002/adma.201907976>.
- (72) Bhargava, S. S.; Azmoodeh, D.; Chen, X.; Cofell, E. R.; Esposito, A. M.; Verma, S.; Gewirth, A. A.; Kenis, P. J. A. *Decreasing the Energy Consumption of the CO₂ Electrolysis Process Using a Magnetic Field. ACS Energy Lett.* **2021**, 6 (7), 2427–2433. <https://doi.org/10.1021/acsenenergylett.1c01029>.
- (73) Landrum, G. A.; Dronskowski, R. *The Orbital Origins of Magnetism: From Atoms to Molecules to Ferromagnetic Alloys. Angew. Chemie Int. Ed.* **2000**, 39 (9), 1560–1585. [https://doi.org/10.1002/\(SICI\)1521-3773\(20000502\)39:9<1560::AID-ANIE1560>3.0.CO;2-T](https://doi.org/10.1002/(SICI)1521-3773(20000502)39:9<1560::AID-ANIE1560>3.0.CO;2-T).
- (74) Mravlje, J.; Aichhorn, M.; Georges, A. *Origin of the High Néel Temperature in $\text{SrTcO}_{3-\text{Mn}}$. Phys. Rev. Lett.* **2012**, 108 (19), 197202. <https://doi.org/10.1103/PhysRevLett.108.197202>.
- (75) Montoya, J. H.; Doyle, A. D.; Nørskov, J. K.; Vojvodic, A. *Trends in Adsorption of Electrocatalytic Water Splitting Intermediates on Cubic ABO₃ Oxides. Phys. Chem. Chem. Phys.* **2018**, 20 (5), 3813–3818. <https://doi.org/10.1039/C7CP06539F>.
- (76) Nørskov, J. K.; Bligaard, T.; Logadottir, A.; Kitchin, J. R.; Chen, J. G.; Pandelov, S.; Stimming, U. *Trends in the Exchange Current for Hydrogen Evolution. J. Electrochem. Soc.* **2005**, 152 (3), J23. <https://doi.org/10.1149/1.1856988>.
- (77) Balandin, A. A. Modern State of the Multiplet Theor of Heterogeneous Catalysis. In *Advances in Catalysis*; 1969; Vol. 19, pp 1–210. [https://doi.org/10.1016/S0360-0564\(08\)60029-2](https://doi.org/10.1016/S0360-0564(08)60029-2).
- (78) Jaksic, J. M.; Ristic, N. M.; Krstajic, N. V.; Jaksic, M. M. *Electrocatalysis for Hydrogen Electrode Reactions in the Light of Fermi Dynamics and Structural Bonding FACTORS—I. Individual Electrocatalytic Properties of Transition Metals. Int. J. Hydrogen Energy* **1998**, 23 (12), 1121–1156. [https://doi.org/10.1016/S0360-3199\(98\)00014-7](https://doi.org/10.1016/S0360-3199(98)00014-7).
- (79) Hammer, B.; Nørskov, J. K. Theoretical Surface Science and Catalysis—Calculations and

- Concepts. In *Advances in Catalysis*; 2000; Vol. 45, pp 71–129. [https://doi.org/10.1016/S0360-0564\(02\)45013-4](https://doi.org/10.1016/S0360-0564(02)45013-4).
- (80) Vojvodic, A.; Nørskov, J. K.; Abild-Pedersen, F. *Electronic Structure Effects in Transition Metal Surface Chemistry. Top. Catal.* **2014**, 57 (1–4), 25–32. <https://doi.org/10.1007/s11244-013-0159-2>.
 - (81) Trasatti, S. *Work Function, Electronegativity, and Electrochemical Behaviour of Metals. J. Electroanal. Chem. Interfacial Electrochem.* **1972**, 39 (1), 163–184. [https://doi.org/10.1016/S0022-0728\(72\)80485-6](https://doi.org/10.1016/S0022-0728(72)80485-6).
 - (82) Hong, W. T.; Welsch, R. E.; Shao-Horn, Y. *Descriptors of Oxygen-Evolution Activity for Oxides: A Statistical Evaluation. J. Phys. Chem. C* **2016**, 120 (1), 78–86. <https://doi.org/10.1021/acs.jpcc.5b10071>.
 - (83) Han, B.; Risch, M.; Lee, Y.-L.; Ling, C.; Jia, H.; Shao-Horn, Y. *Activity and Stability Trends of Perovskite Oxides for Oxygen Evolution Catalysis at Neutral PH. Phys. Chem. Chem. Phys.* **2015**, 17 (35), 22576–22580. <https://doi.org/10.1039/C5CP04248H>.
 - (84) Jiao, Y.; Sharpe, R.; Lim, T.; Niemantsverdriet, J. W. H.; Gracia, J. *Photosystem II Acts as a Spin-Controlled Electron Gate during Oxygen Formation and Evolution. J. Am. Chem. Soc.* **2017**, 139 (46), 16604–16608. <https://doi.org/10.1021/jacs.7b07634>.
 - (85) Gracia, J. *Itinerant Spins and Bond Lengths in Oxide Electrocatalysts for Oxygen Evolution and Reduction Reactions. J. Phys. Chem. C* **2019**, 123 (15), 9967–9972. <https://doi.org/10.1021/acs.jpcc.9b01635>.
 - (86) Xiong, Q.; Wang, Y.; Liu, P.-F.; Zheng, L.-R.; Wang, G.; Yang, H.-G.; Wong, P.-K.; Zhang, H.; Zhao, H. *Cobalt Covalent Doping in MoS₂ to Induce Bifunctionality of Overall Water Splitting. Adv. Mater.* **2018**, 30 (29), 1801450. <https://doi.org/10.1002/adma.201801450>.
 - (87) Xiang, Z.; Zhang, Z.; Xu, X.; Zhang, Q.; Wang, Q.; Yuan, C. *Room-Temperature Ferromagnetism in Co Doped MoS₂ Sheets. Phys. Chem. Chem. Phys.* **2015**, 17 (24), 15822–15828. <https://doi.org/10.1039/C5CP01509J>.
 - (88) Goodenough, J. B. *Electronic and Ionic Transport Properties and Other Physical Aspects of Perovskites. Reports Prog. Phys.* **2004**, 67 (11), 1915–1993. <https://doi.org/10.1088/0034-4885/67/11/R01>.
 - (89) Gracia, J.; Biz, C.; Fianchini, M. *The Trend of Chemisorption of Hydrogen and Oxygen Atoms on Pure Transition Metals: Magnetism Justifies Unexpected Behaviour of Mn and Cr. Mater. Today Commun.* **2020**, 23, 100894. <https://doi.org/10.1016/j.mtcomm.2020.100894>.
 - (90) Gracia, J. *Spin Dependent Interactions Catalyse the Oxygen Electrochemistry. Phys. Chem. Chem. Phys.* **2017**, 19 (31), 20451–20456. <https://doi.org/10.1039/C7CP04289B>.
 - (91) Felser, C.; Fecher, G. H.; Balke, B. *Spintronics: A Challenge for Materials Science and Solid-State Chemistry. Angew. Chemie Int. Ed.* **2007**, 46 (5), 668–699. <https://doi.org/10.1002/anie.200601815>.

For Table of Contents Only

